



MAGNETOCONVECTION AND IRREVERSIBILITY PHENOMENA WITHIN A LID DRIVEN CAVITY FILLED WITH LIQUID METAL UNDER MAGNETIC FIELD

Fakher Oueslati^{a, b, †}, Brahim Ben-Beya^b

^a Physics Department, Faculty of Science Albaha, Albaha University, 6543 Al-Baha, Kingdom of Saudi Arabia

^b Laboratory of Physics of Fluids, Physics Department, Faculty of Science of Tunis, University of Tunis El-Manar, 2092 El-Manar 2, Tunis, Tunisia

ABSTRACT

The current study deals with a numerical investigation of magnetoconvection and entropy generation within a lid driven square cavity subject to uniform magnetic field and filled with liquid metal. Effects of multiple parameters namely; the Prandtl, Hartmann and Richardson numbers were predicted and analyzed using a numerical methodology based on the finite volume method and a full multigrid technique. The numerical outcome of the present study shows that, the enhancement of Hartmann number declines the heat transfer rate for all liquid metals considered. Moreover, it is observed that augmenting the Richardson number leads to acceleration of the flow with a centro-symmetry for both velocity components. In terms of irreversibility phenomena, it is found that contrarily to the Hartmann parameter, enhancing the Richardson values leads to strengthening the entropy generation rates within the cavity especially for relatively highest values. The comparison of three situations of moving lids considered shows that the case where both horizontal walls are moving in opposite directions appears to strengthen the heat transfer and entropy generation within the cavity.

Keywords: *Magnetic field; Mixed convection; Entropy generation; Heat transfer; Lid-driven cavity*

1. INTRODUCTION

To Natural convection analysis in lid-driven cavities is one of the most widely studied problems in thermo-fluids areas. A great number of researches have been carried out in the past decades on cavities having one or more moving lids considering different combinations cavity shapes or imposed boundary conditions (Botella and Peyret, 1998; Erturk, 2009; Ouertatani *et al.*, 2009; Lin *et al.*, 2011; Abu-Nada, 2015). On another hand, the mixed convection heat transfer and fluid flow in confined cavities in the presence of magnetic fields has also received considerable attention in recent years due to possible applications in many technological and industrial fields such as fusion reactors, crystal growth cooling of electronic systems, chemical processing equipment, and solar collectors (Oreper and Szekely, 1983; Naffouti *et al.*, 2014; Kherief *et al.* 2012). In fact, numerous studies have analyzed the effect of applying external magnetic fields on convective heat transfer rate. In addition, a great interest has been paid to magneto-hydrodynamics (MHD) natural convection in the presence of liquid metals by applying magnetic field to control convection electrically low-conducting fluids, such as the melt of inorganic oxides and aqueous solutions of salts or semiconductor melts such as silicon (Mohamad and Viskanta 1994; Wang and Wakayama, 2002; Yazdi *et al.*, 2014, Kolsi, 2016; Al-Rashed *et al.*, 2017). For instance, in the natural convection case, Al-Mudhaf and Chamkha (2004) predicted the magneto-hydrodynamics (MHD) natural convection of electrically conducting liquid metals such as gallium and germanium in an inclined rectangular enclosure in the presence of a uniform magnetic field. It was found that, in the absence of a magnetic field, a three-cellular structure exists while this pattern does not exist for relatively weak Hartmann number values where a single vortex structure dominates. In addition, it was seen that exact tilt angle for which the average Nusselt

number decreases or increases depended on the values of the fluid Prandtl and Rayleigh numbers for the fixed value of Hartmann parameter considered. A numerical study of natural convection flow of electrically conducting liquid gallium in a square cavity at which a uniform magnetic field inclined at an angle is externally imposed, was carried out by Sathiyamoorthy and Chamkha (2010). The authors demonstrated that the magnetic field with inclined angle has effects on the fluid flow and heat transfer rates in the cavity. It was also found that the average Nusselt number decreases non-linearly by increasing Hartmann number for any inclined angle. The magnetic field influence on natural convection of non-Newtonian power-law fluids in a sinusoidal heated cavity was predicted by Kefayati (2014). The numerical simulation was carried out for a magnetic field applied at different inclinations angle and for various Rayleigh and Hartmann numbers as well as power-law index values. The author demonstrated that the amount of the magnetic field affects in general the heat transfer rate and the fluid flow field was seen to be different in the vertical and horizontal ones. Furthermore, Mahmoudi *et al.* (2014) used the Lattice Boltzmann method to simulate the MHD natural convection in a nanofluid-filled cavity with linear temperature distribution when the magnetic field is varied. It was stated that for specific values of Rayleigh and Hartmann number, the heat transfer rate and fluid flow depend strongly on the direction of magnetic field. In addition, according to the Hartmann number, it was seen that the magnetic field direction controls the effects of nanoparticles.

Although the available literature on magnetoconvection in confined is numerous, the corresponding research utilizing moving lids is quite sparse. For instance, Oztop *et al.* (2011) implemented the Finite Volume method to investigate the MHD mixed convection in a lid-driven cavity having a corner heater. These authors demonstrated that the thermal boundary layer becomes higher with increasing of Hartmann number and isotherms fit with the corner, while the heat

[†] Corresponding author. Email: fakher.oueslati@gmail.com

transfer decreases with increasing of the Hartmann number values. In addition, Farid *et al.* (2013) carried out a numerical study of the MHD mixed convection in a lid driven enclosure with circular heated hollow cylinder. It was shown that flow velocity as well as the heat transfer rate is reduced with augmenting of Hartmann number. Besides, thinner thermal boundary layer was observed for lower values of Ha values, while strengthened thermal transfer rate was obtained for lower ones.

Kefayati (2015) studied the influence of the application of a magnetic field on the mixed convection of shear-thinning fluids in a square lid-driven cavity with sinusoidal boundary conditions using finite difference lattice Boltzmann method. It was seen that the enhancement of Hartmann parameter declines heat and mass transfer rates for different buoyancy ratios and power-law indexes steadily at $Ri = 0.00062$ and 0.01 . Furthermore, it was observed that the increase of Lewis number enhances the mass transfer rate for the studied Hartmann and buoyancy ratio values. In another contribution, using the same numerical technique, Kefayati (2015) predicted the laminar mixed convection of non-Newtonian nanofluids in a two sided lid-driven cavity filled with water and nanoparticles in the presence of a horizontal magnetic. He highlighted that the growing of Richardson number decreases the heat transfer and that the fall of the power law index declines it. Besides, the author stated that the increase in Hartmann number drops the heat transfer generally and also affects the power-law index and nanoparticle influences on mixed convection phenomenon.

The above investigations all are based on the first-law of thermodynamics. However, to further improve the MHD convection, optimization based on the second-law of thermodynamics is compulsory. During the past three decades, entropy generation analysis has become a powerful tool to optimize various complicated systems. For instance, multiple studies predicted the irreversibility phenomenon within confined cavities. In this context, Mahmoudi *et al.* (2014) used the Lattice Boltzmann technique to numerically analyze the natural convection in a square enclosure filled with nanofluid in the presence of magnetic field and uniform heat generation/absorption. The results show that the heat generation/absorption coefficient influences heat transfer rate, whereas it does not influence the entropy generation for specific parameters. Moreover, it was seen that adding nanoparticle diminished the entropy generation especially for higher values of Hartmann number. Mehrez *et al.* (2015) carried out a numerical prediction to investigate the effect of an external oriented magnetic field on heat transfer and entropy generation of Cu-water nanofluid flow in an open cavity heated from below. The results demonstrated that the entropy generation, the fluid flow behavior as well as the heat transfer rate are strongly affected by the presence of a magnetic field. Furthermore, it was shown that thermal rate and irreversibility criterion depend on the Richardson and Reynolds numbers while applying a magnetic field or adding nanoparticles. Very recently, the heat transfer and entropy generation due to laminar natural convection in a square cavity filled with non-Newtonian nanofluid has been analyzed by Kefayati (2015) using the Finite Difference Lattice Boltzmann Method. The author declared that the entropy generation due to fluid friction and heat transfer augments as the Rayleigh number value increases. In addition, he observed that strengthening the volume fraction enhances both the entropy generations due to heat transfer and to fluid friction in different power-law indexes.

As shown by the above comprehensive literature conveys, and to the best knowledge of the authors, until now, there are no open studies available yet on entropy generation of MHD convection for the case of lid driven cavities. Furthermore, less attention has been attributed to lid-driven cavity filled with a liquid metals. From this point of view, the current investigation aims to analyze the magnetoconvection and irreversibility phenomena within cavity filled with liquid metals for different cases of moving lids. The study is conducted numerically for various mainly governing parameters, whose effects upon the flow patterns, entropy generation, the temperature distributions and the thermal rate are discussed and analyzed.

2. PHYSICAL MODEL AND FORMULATION

2.1 Physical model and governing equations

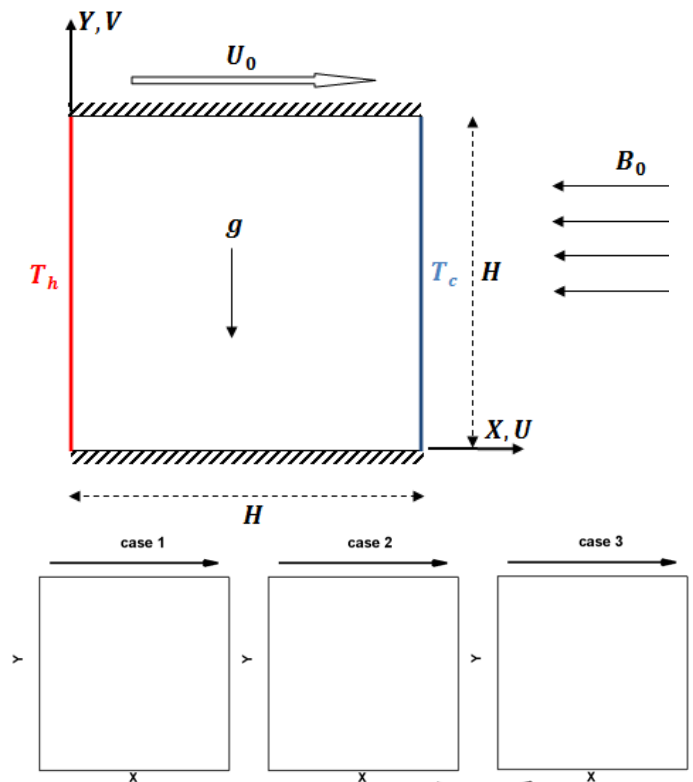


Fig. 1 Physical model with active side walls for the three investigated cases of the lid driven cavity.

The physical model consists of a two-dimensional square cavity of height H and filled with a liquid metal in the presence of a uniform magnetic field B_0 as schematically illustrated in Fig. 1. Note that the uniform magnetic field B_0 is applied to the fluid in the normal direction to Y . The dimensionless Cartesian coordinates (X, Y) , and the boundary conditions are indicated herein. Gravity acts in the negative Y -direction. The temperatures T_h and T_c are uniformly imposed on two opposing walls such that $T_h > T_c$ while the other two walls are assumed to be adiabatic. In the current study, three situations of moving lid will be considered as shown in Fig. 1. The first case corresponds to the situation where only the top wall is moving in the X -direction with constant velocity U_0 (case 1). The second case describes the situation of lid driven cavity animated by the two horizontal walls moving in the same direction (case 2). The third case corresponds to the situation where both horizontal walls move in opposite directions (case 3). It is worth noting that ten liquid metals are considered in the current investigations and the corresponding Prandtl numbers are listed in Table 1.

In the current study, all thermophysical properties of the fluid are supposed to be constant except for the density variation in the buoyancy term, where the Boussinesq approximation is adopted as:

$$\rho = \rho_0[1 - \beta(T - T_c)] \quad (1)$$

where ρ_0 is the fluid density at the reference temperature T_0 and $\beta = -(1/\rho_0)(\partial\rho/\partial T)$ is the thermal expansion coefficient.

Furthermore, we assumed that radiation mode of heat transfer, Joule heating and Hall effects are neglected according to other modes of heat transfer. By employing the aforementioned assumptions, the governing equations can be expressed in their dimensionless form as follows:

$$\frac{\partial U}{\partial X} + \frac{\partial V}{\partial Y} = 0 \quad (2)$$

$$\frac{\partial U}{\partial t} + U \frac{\partial U}{\partial X} + V \frac{\partial U}{\partial Y} = -\frac{\partial P}{\partial X} + \frac{1}{\text{Re}} \left(\frac{\partial^2 U}{\partial X^2} + \frac{\partial^2 U}{\partial Y^2} \right) \quad (3)$$

$$\frac{\partial V}{\partial t} + U \frac{\partial V}{\partial X} + V \frac{\partial V}{\partial Y} = -\frac{\partial P}{\partial Y} + \frac{1}{\text{Re}} \left(\frac{\partial^2 V}{\partial X^2} + \frac{\partial^2 V}{\partial Y^2} \right) + \text{Ri}\theta - \frac{Ha^2}{\text{Re}} V \quad (4)$$

$$\frac{\partial \theta}{\partial t} + U \frac{\partial \theta}{\partial X} + V \frac{\partial \theta}{\partial Y} = \frac{1}{\text{Pr}\cdot\text{Re}} \left(\frac{\partial^2 \theta}{\partial X^2} + \frac{\partial^2 \theta}{\partial Y^2} \right) \quad (5)$$

The dimensionless quantities $X_i=(X, Y)$, $U_i=(U, V)$, t, P or θ denote the coordinates space, velocity component in the X_i direction, time, pressure and temperature, respectively. The governing equations (1-4) are non-dimensionalized using scales $H, \alpha/H, H^2/\alpha, \rho U_0^2$ and ΔT for coordinate space, velocity, time, pressure and temperature respectively, where $U_0 = \alpha/H$ and ΔT is expressed as: $\Delta T = T_h - T_c$.

The dimensionless temperature is defined as $\theta = (T - T_c) / \Delta T$. The above system of equations introduce the following dimensionless parameters; $\text{Pr} = \nu / \alpha$, $Ha = B_0 H \sqrt{\sigma / \rho \nu}$, $\text{Re} = U_0 H / \nu$, $Gr = g\beta(T_h - T_c)H^3 / \nu^2$, $Ri = Gr / \text{Re}^2$ denoting the Prandtl, Hartmann, Reynolds, Grashof and Richardson numbers, respectively. Here ν is the kinematic viscosity of the fluid, α is the thermal diffusivity, σ is the electrical conductivity, and g is the acceleration due to gravity.

On the solid walls no-slip boundary conditions were imposed. The relevant boundary conditions, if we consider the (case 1) where only the top wall is animated, are given as follows:

- On the top wall ($Y = 1$): $U = 1$, and $\frac{\partial \theta}{\partial X} = 0$
- On the bottom wall ($Y = 0$): $U = 0$, and $\frac{\partial \theta}{\partial X} = 0$
- At the right wall ($X = 1$): $\theta = 0$, and $U = V = 0$
- At the left wall ($X = 0$): $\theta = 1$, and $U = V = 0$

The rate of heat transfer is computed at the left hot wall and is expressed in terms of the local Nusselt number as $Nu = -\frac{\partial \theta}{\partial Y} \Big|_{X=0}$.

The resulting average Nusselt number is then defined as

$$\overline{Nu} = \int_0^1 Nu dY \quad (6)$$

2.2 Equations for entropy generation

In MHD natural convection problem, the associated irreversibilities are due to heat transfer and fluid friction. According to local thermodynamic equilibrium of linear transport theory (Zahmatkesh 2008; Mukhopadhyay, 2010; Kolsi *et al.*, 2014; Magherbi *et al.*, 2006), the dimensionless form of local entropy generation S^{loc} due to heat transfer S_{th}^{loc} and to fluid friction S_{fr}^{loc} for a two-dimensional heat and fluid flow is given by:

$$S^{loc} = S_{th}^{loc} + S_{fr}^{loc} \quad (7)$$

where S_{th}^{loc} and S_{fr}^{loc} are expressed by:

$$S_{th}^{loc} = \left[\left(\frac{\partial \theta}{\partial X} \right)^2 + \left(\frac{\partial \theta}{\partial Y} \right)^2 \right] \quad (8)$$

$$S_{fr}^{loc} = \varphi \left[2 \left(\frac{\partial U}{\partial X} \right)^2 + 2 \left(\frac{\partial V}{\partial Y} \right)^2 + \left(\frac{\partial U}{\partial Y} + \frac{\partial V}{\partial X} \right)^2 \right] \quad (9)$$

where φ denotes the irreversibility coefficient ratio defined by :

$$\varphi = \frac{\mu T_0}{k} \left(\frac{\nu}{H \Delta T} \right)^2 \quad (10)$$

which is taken constant at $\varphi = 0.01$ in the present investigation.

The dimensionless total entropy generation S_{tot} in the enclosure is given by the summation of the total entropy generation due to heat transfer S_{th} and fluid friction S_{fr} which in turn are obtained via integrating the local entropy generation rates S_{th}^{loc} and S_{fr}^{loc} over the domain Ω :

$$S_{tot} = \int_{\Omega} S^{loc} d\Omega = \int_{\Omega} S_{th}^{loc} d\Omega + \int_{\Omega} S_{fr}^{loc} d\Omega = S_{th} + S_{fr} \quad (11)$$

Another dimensionless parameter is considered which is the Bejan number Be representing the ratio of heat transfer irreversibility to the total irreversibility due to heat transfer and fluid friction and defined as:

$$Be = \frac{S_{th}}{S_{th} + S_{fr}} \quad (12)$$

3. NUMERICAL TECHNIQUE AND VALIDATION

3.1 Numerical methodology

The dimensionless Navier-Stokes equations were numerically solved using the following numerical methodology. The temporal discretization of the time derivative is performed by an Euler backward second-order implicit scheme. Non linear terms are evaluated explicitly; while, viscous terms are treated implicitly. The strong velocity–pressure coupling present in the continuity and the momentum equations is handled by implementing the projection method (Brown *et al.*, 2001). A Poisson equation, with the divergence of the intermediate velocity field as the source term, is then computed to obtain the pressure correction and the real velocity field. We have also used a finite volume method on a staggered grid system in order to discretize the system of equations to be solved. The QUICK scheme of Hayase *et al.* (1992) is implemented to minimize the numerical diffusion for the advective terms. The Poisson equation which is solved using an accelerated full multigrid method (Ben-Cheikh *et al.*, 2007), while the discretized equations are computed using the red and black point successive over-relaxation method (Hadjidimos, 2000) with the choice of optimum relaxation factors. Finally, the convergence of the numerical results is established at each time step according to the following criterion:

$$\max \left(\left| \frac{\Phi_{i,j}^{m+1} - \Phi_{i,j}^m}{\Phi_{i,j}^m} \right| \right) \leq 10^{-8} \quad (13)$$

The generic variable Φ stands for U, V, P or θ and, m indicates the iteration time levels. In the above inequality, the subscript sequence (i, j) represents the space coordinates X and Y .

Simulations were performed by using a developed home code named “NASIM” (Ben-Beya and Lili, 2009; Oueslati *et al.*, 2011; Oueslati *et al.*, 2013; Oueslati *et al.*, 2014; Oueslati *et al.*, 2014; Oueslati *et al.*, 2015) using finite volume method and the numerical procedure described above. It is worth noting that all simulations of the present study were conducted with non-uniform grids of 128^2 .

Furthermore, due to the presence of large gradients near the moving lids, we have chosen to generate a centro-symmetric grid with clustering near the walls using the following n grid point distribution:

$$X_i = \frac{1}{2} \left(1 + \frac{\tanh[\xi(2i/n-1)]}{\tanh(\xi)} \right) \quad (14)$$

where $\xi = 1.25$ and $1 \leq i \leq n$. Similar grid point distribution has been used in the both directions of the cavity.

3.2 Code validation

Table 1 Different liquid metals considered with corresponding Prandtl number values

Metal	Symbol	Prandtl
Sodium	Na	0.0051
Potassium	K	0.0066
Germanium	Ge	0.0070
Tin	Sn	0.0110
Lead	Pb	0.0130
Bismuth	Bi	0.0142
Aluminum	Al	0.0150
NaK-alloy	NaK	0.0213
Mercury	Hg	0.0248
Gallium	Ga	0.0250

Table 2 Comparison of \overline{Nu} obtained with the present code with those from literature for $Gr = 2.10^4$

Ha	P. study	Sathiyamoorthy and Chamkha (2012)	%	Rudraiah <i>et al.</i> (1995)	%	Sheikholeslami <i>et al.</i> (2013)	%
0	2.5018	2.5439	1.654	2.5188	0.674	2.5665	2.52
10	2.2130	2.2385	1.139	2.2234	0.467	2.2662	2.35
100	1.0063	1.0066	0.029	1.0110	0.464	1.0221	1.553

Table 3 Numerical computations of the average Nusselt values obtained with the present simulations with those of Al-Mudhaf and Chamkha (2004) for the case of cavity filled with liquid gallium ($Pr=0.025$) and inclined with 45° at $Ra = 10^4$.

Ha	\overline{Nu}	
	Al-Mudhaf and Chamkha (2004)	Present study
50	1.86365	1.812094 (2.766 %)
70	1.42970	1.38965 (2.801 %)
100	1.13567	1.120809 (1.308 %)

Before proceeding with numerical simulations in the case of the cavity filled with a liquid metal and subjected to the magnetic field, a first validation of the in-house code "NASIM" was conducted for the case of magnetoconvection. To do so, the numerical results of the average Nusselt values of this study are compared with those obtained by Sathiyamoorthy and Chamkha (2012), of Rudraiah *et al.* (1995) and also to the computations of Sheikholeslami *et al.* (2013) for the case of a square enclosure filled with air ($Pr = 0.71$). It should be noted that the

corresponding results are obtained with a grid of 48^2 and a Grashof number $Gr = 2 \times 10^4$. As shown in Table 2 a good agreement between the results of this calculation code and those from literature is observed with a maximum relative error of about 2%.

Furthermore, a second validation of our numerical simulations was carried out for the case of magnetoconvection in an inclined rectangular cavity of aspect ratio 2 and filled with liquid gallium ($Pr = 0.025$) corresponding to the case investigated by Al-Mudhaf and Chamkha (2004). The \overline{Nu} values predicted by the present code listed in Table 3 are given for a Rayleigh number value $Ra = Gr \times Pr = 10^4$ and an inclination angle of 45° with respect to Hartmann number values $Ha = 50, 70$ and 100 . As we can clearly see from this table, a good agreement is still found, which once again demonstrates the robustness of this code.

On another hand, and in order to demonstrate the performance of our code, we carried out a validation of our numerical simulations for the case of mixed convection with those obtained by Iwatsu *et al.* (1993) and Cheng (2011). The adopted configuration is a square cavity filled with air in which the upper wall is heated and animated while the lower one is kept cooled. It should be noted that the corresponding results are obtained with a grid of 128^2 for different values of the Grashof number $Gr = Ra/Pr$. As depicted in Table 4, a fair agreement between the results of this calculation code and those in the literature are observed again. These validations make a good confidence in the present numerical code.

Table 4 Comparison of the results of the present code with those obtained by Iwatsu *et al.* (1993) and Cheng (2011) for different Grashof values.

Re	References	Gr		
		10^2	10^4	10^6
400	Present study	4.12	3.89	1.20
	Iwatsu <i>et al.</i> (1993)	3.84	3.62	1.22
	Cheng (2011)	4.14	3.90	1.21
1000	Present study	6.79	6.73	1.82
	Iwatsu <i>et al.</i> (1993)	6.33	6.29	1.77
	Cheng (2011)	6.73	6.68	1.75

4. RESULTS AND DISCUSSION

4.1 Influence of Ha and Pr for the cavity filled with different liquid metals

In order to understand the influence of Hartmann number which measures the force magnetic field on heat transfer in the lid-driven cavity filled a liquid metal, we illustrate in Fig. 2 the profiles variations of the average Nusselt number as function of the Hartmann parameter as well as the corresponding histograms for different number of Prandtl. Note that in this section we only consider the first case (case 1) illustrated in Fig. 1 describing the cavity where only the top wall is animated for $Re=400$ and $Ri=100$.

As seen in Fig. 2, in addition to the control of the hydrodynamic (velocities), the magnetic field influence on the flow structures and thermal field is manifested generally by deceleration of the heat transfer rate. In fact, and for all the liquid metals, increasing the number of Hartmann causes monotonic decrease in average Nusselt values reflecting the ratio of total heat transfer by the thermal transfer rate due to conduction. The cause of this decrease experienced by the heat transfer rate is due to the presence of thermal buoyancy forces in

addition to the imposed magnetic field. In fact, this force acts in the opposite direction of flow which causes the reduction of the convective effect within the cavity. In other words, when the Hartmann number Ha increases, the magnitude order of magnetic force increases and, consequently, the intensity of the convective flow is hence reduced. On the other hand, histograms illustrated in Fig. 2 (b) shows that the most strengthened heat transfer rates are obtained for highest Prandtl numbers values. As shown in both figures, an increase of the Prandtl number is expressed by an improvement in the value of average Nusselt number where the maximum rate is obtained for the gallium which is the liquid metal corresponding to the greater value of Pr considered.

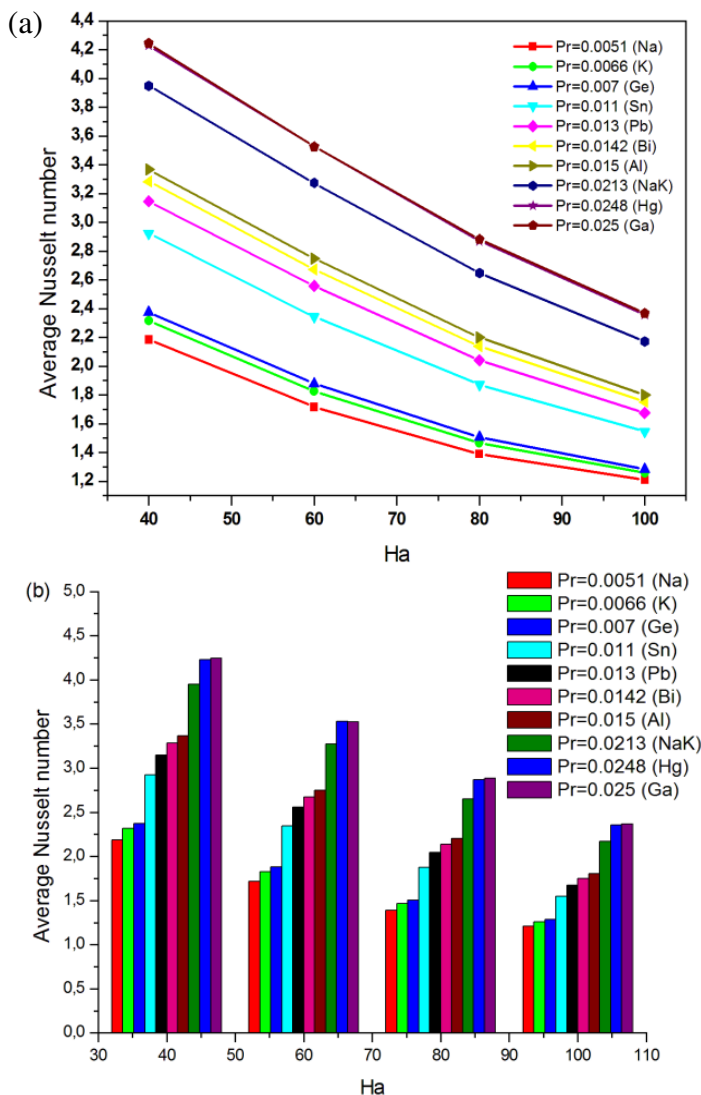


Fig. 2 Evolution of average Nusselt number profiles as a function of Ha with corresponding histograms for different Prandtl number: (a) variations of \bar{Nu} according to Ha and (b) corresponding histograms.

4.2 Case of cavity filled with liquid gallium

Effect of the Hartmann number

In this section we propose to predict the effect of multiple parameters for the case of cavity filled with liquid gallium ($Pr=0.025$), which corresponds to the liquid metal giving the optimum of heat transfer rate as previously shown. Note that we still adopt the case of the enclosure where only the top wall is animated (case 1) with respect to fixed parameters $Ra = 4 \times 10^5$, $Gr = Ra / Pr = 1.6 \times 10^7$, $Re=400$ and $Ri=100$.

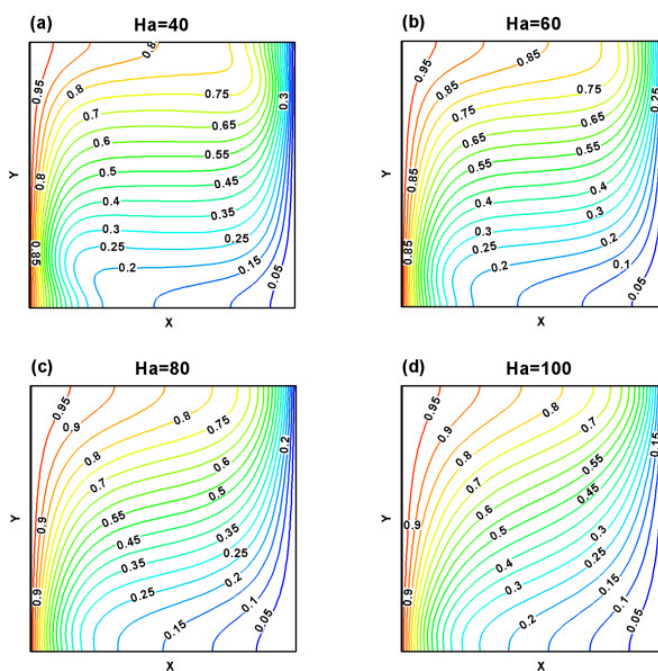


Fig. 3 Isothermal structures in the cavity filled with liquid gallium for different Hartmann number corresponding to the Richardson number value $Ri = 100$: (a) $Ha = 40$, (b) $Ha = 60$, (c) $Ha = 80$ and (d) $Ha = 100$.

In Fig. 3 are plotted the isothermal structures for various Hartmann number values corresponding to steady states, namely; $Ha=40, 60, 80$ and 100 . Examination of Fig. 3 indicates the dominance of the conductive regime when the Hartmann number strengthens especially for $Ha = 80$ and 100 . This is shown by the thermal stratification described by isotherms that are deformed more and more and become almost parallel to the vertical walls. This is in good agreement with the Nusselt profile trends analyzed in Fig. 2 indicating that augmenting the magnitude of the magnetic field, meaning increasing the Ha value, has the tendency to decelerate the heat transfer rate in the enclosure filled with liquid gallium. On another hand, Fig. 4 illustrates a comparison of the projection of the fluid particle trajectories for both values of the Hartmann number $Ha = 40$ and 100 . For the minimum value of Hartmann number $Ha= 40$, the flow is described by the presence of a primary vortex with two secondary ones turning counterclockwise. With a close scrutiny of the flow structures, we may also see the birth of fluid trajectory deformations at the vicinity of the four cavity corners, which may be due to the driving effect of the top wall. Indeed, it is generally known that in the case of lid-driven cavities, instabilities may arise due to the Taylor Gortler vortices that are responsible for such distortions near the corners. By rising the Hartmann number value up to $Ha=100$, the two secondary vortices merge and form a primary roll which occupies most part of the cavity describing the classical circulating of natural convection flow.

Influence of the Richardson number

In this section, we intend to highlight the effect of the Richardson number Ri on the flow pattern and heat transfer rate in the lid-driven cavity filled with liquid gallium. The simulations were conducted for Ri values in a range of $Ri=0.01, 0.1, 1, 10$ and 100 for the fixed parameters $Ha= 100, Re=400$ and $Pr=0.025$.

Profile variations of the U and V -maximum velocity components are depicted in Fig.6. As illustrated by this figure, the circulating flow intensity has significantly increased; this is shown by the speed acceleration of the liquid metal in the enclosure. This seems to be in accordance with the velocity evolution profiles previously discussed in

Fig. 5 demonstrating that augmenting the Richardson number leads to intensifying the flow velocity.

In order to further predict the influence of Richardson parameter on the general flow structure, in Fig. 7 we illustrate the fluid particle trajectories for $Ri=0.1, 1, 10$ and 100 by fixing both parameters Ha and Pr at $Ha = 100$ and $Pr = 0.025$. For $Ri = 0.1$, we note the presence of three recirculation rolls, a primary vortex occupying the lower half side and two secondary vortices that develop near the top moving wall. By reaching the unit value ($Ri=1$), one of the second roll disappears and the main vortex gains more volume. By increasing the value of Ri , and from $Ri=10$, the two vortices seem to merge until reaching $Ri = 100$ where a single vortex counterclockwise rotation occupies the whole volume of the cavity.

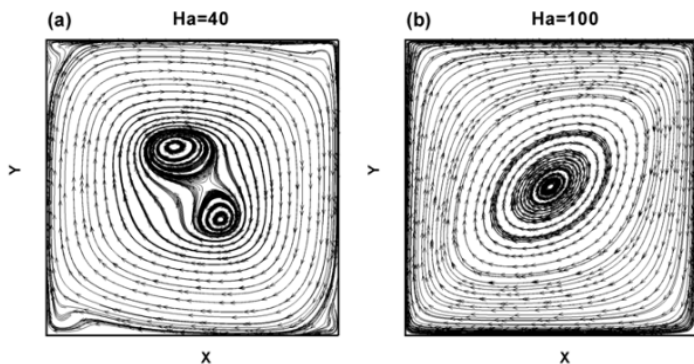


Fig. 4 Trajectory of fluid particles for the extrema values of the Hartman number $Ha = 40$ (left) and 100 (right) for $Ri=100$ and $Pr = 0.025$: (a) $Ha = 40$, (b) $Ha= 100$.

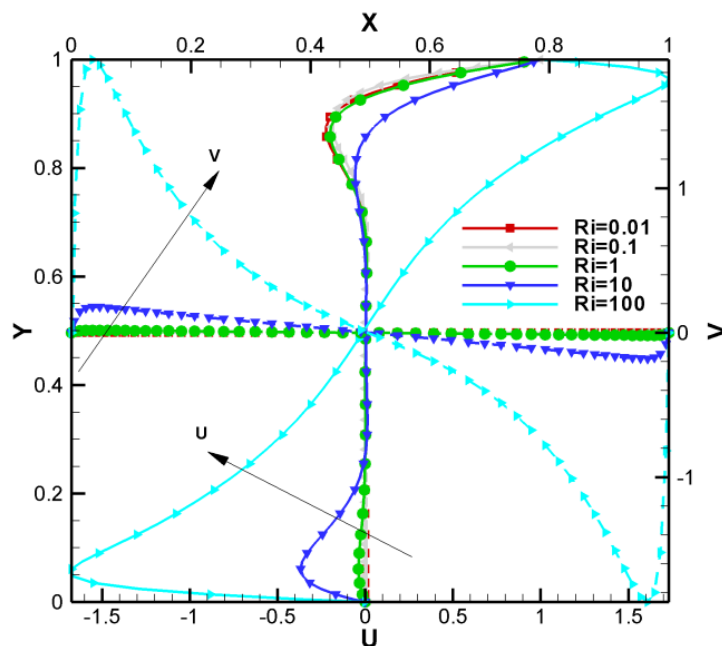


Fig. 5 Velocity component profiles (a) $U(Y)$ and (b) $V(X)$ at the mid-height ($Y = 0.5$) and the mid-width ($X=0.5$) which correspond to $Ri=0.01, 0.1, 1$ and 10 , for the fixed parameters $Ha=100, Re=400$ and $Pr=0.025$.

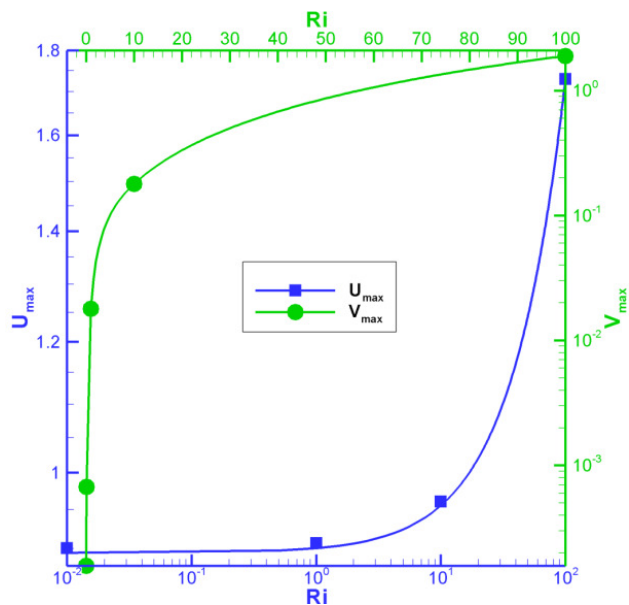


Fig. 6 Velocity maxima variations U_{max} and V_{max} versus the Richardson number for fixed parameters ($Ha = 100$ and $Pr = 0.025$).

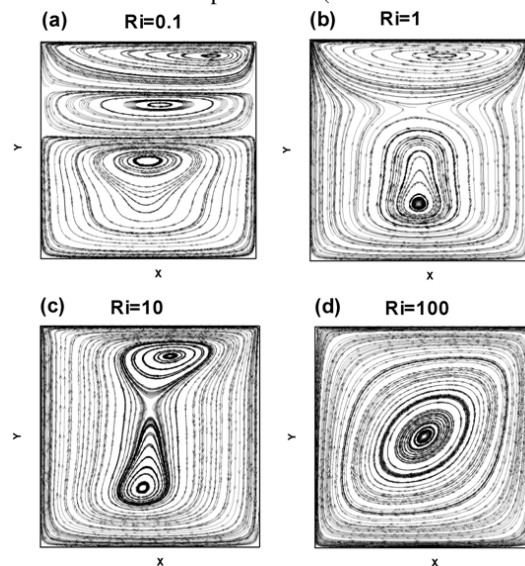


Fig. 7 Stream traces of fluid particles for $Ha=100$ and $Pr=0.025$ with respect to different Richardson number values: (a) $Ri=0.1$, (b) $Ri=1$, (c) $Ri=10$ and (d) $Ri=100$.

In order to understand the Richardson effect on the heat transfer rate within the cavity, we report in Fig. 8 the variation of average Nusselt number with respect to the Richardson parameter values. Examination of this figure demonstrates that the value remains almost fixed to the unit ($\overline{Nu} = 1$) according to fairly small values of Ri ; namely, $Ri = 0.01, 0.1$ and 1 , reflecting the dominance of purely conductive regime. At the value $Ri = 10$, the profile exhibits an exponential growing and peaked at 100 . Thus, based on the numerical results of the magnetoconvection mixed convection in the single lid-driven square enclosure filled with liquid gallium, a correlation of average Nusselt was established as a function of Ri parameter as following

$$\overline{Nu} = e^{(a \times Ri + b)} \quad (15)$$

where a and b are constants given by $a = 8.5126 \times 10^{-3}$ and $b = 8.64646 \times 10^{-3}$

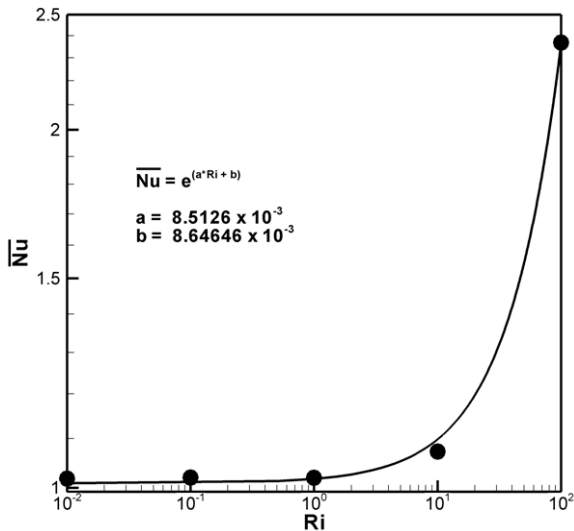


Fig. 8 Profile variation of average Nusselt Number according to Ri for $Ha = 100$, $Re = 400$ and $Pr = 0.025$.

Effect of the Hartmann number on the entropy generation

In this section, we attempt to analyze magnetoconvection mixed convection in terms of irreversibility phenomena generated within the cavity driven by the top wall and filled with liquid gallium ($Pr=0.025$). The results are presented in terms of profiles of total entropy generation and irreversibility isocontours at the steady flow regime. Simulations are predicted for different values of the Hartmann number ($30 \leq Ha \leq 100$) with a step of 10, while the remaining parameters governing the flow are maintained fixed at ($Gr = 1.6 \times 10^7$, $Ri = 100$, and $Re = 400$). To illuminate the effects of Hartmann number on the irreversibility phenomena, profiles of the total entropy generation and the number of Bejan according to the Hartmann parameter are illustrated in Fig. 9. Variations of both total entropy generation due to fluid friction S_{fr} and to heat transfer S_{th} (Fig. 9 (a)) show that the irreversibility rate continues to diminish by further increasing the Hartmann number. On the other hand, the comparison between the two sub-Figs. 9 (a) and 9 (b) indicates that the total production of entropy due to heat transfer is considerably larger than that due to viscosity, which means that entropy generation phenomena are dominated by the irreversible effects due to thermal gradients. This explains the close relative values obtained for the total entropy generation S_{tot} and those of S_{th} easily observed at Fig. 9 (b). Moreover, this figure also discloses reverse evolutions regarding the variations of both Bejan number and total entropy generation S_{tot} . This can be explained by the fact that the dimensionless Bejan number expresses the relative dominance of entropy generation due to heat transfer and fluid friction which induces an evolution inversely proportional to S_{tot} . Figure .10 displays the isocontours of local entropy production due to heat transfer S_{th}^{loc} and S_{fr}^{loc} fluid friction, for selected values of Hartmann number $Ha=40$ and 100 . It is visualized from this typical snapshots that the entropy generation only occurs at the vicinity of the vertical active walls for both values $Ha=40$ and 100 , whereas the rest of the cavity remains stagnant at an equilibrium state. Furthermore, thermal local entropy structures and viscous ones are seen to be symmetrically distributed with respect to the diagonal and having significant values near these zones. By augmenting the Hartmann number, the irreversibility isocontours intensities decrease significantly meaning that the application of magnetic field reduces the effects of entropy generation in the cavity.

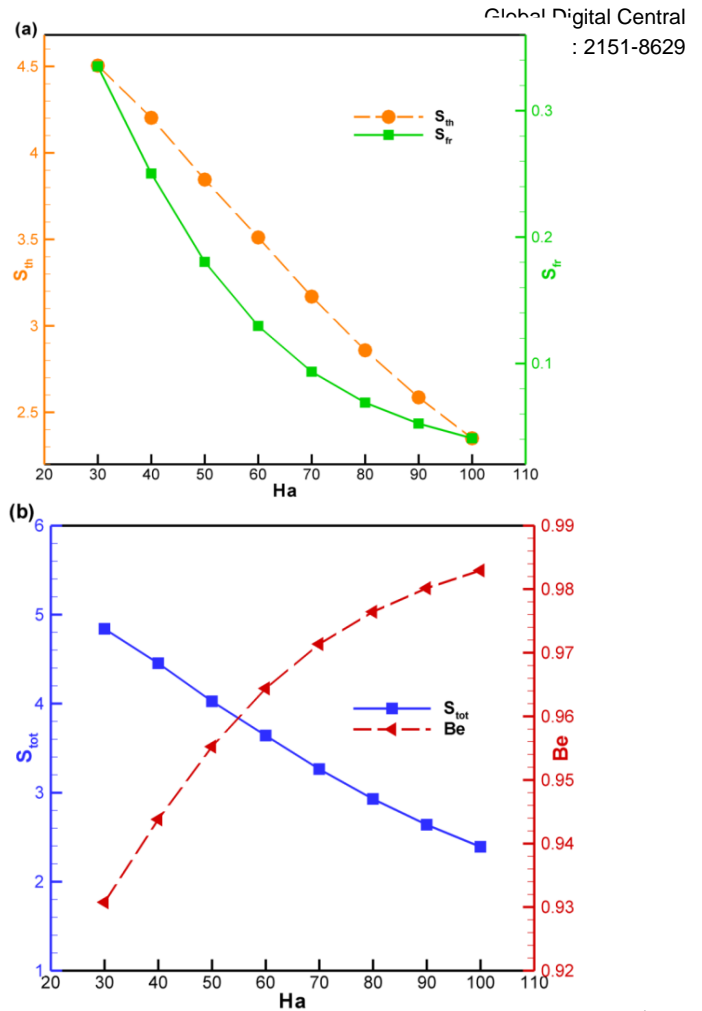


Fig. 9 Variations of total entropy generations versus Hartmann number for $Ri = 100$ and $Pr = 0.025$ (a) profiles of both total entropy generation due to fluid friction S_{fr} and to heat transfer S_{th} , and (b) total entropy generation S_{tot} and Bejan number Be .

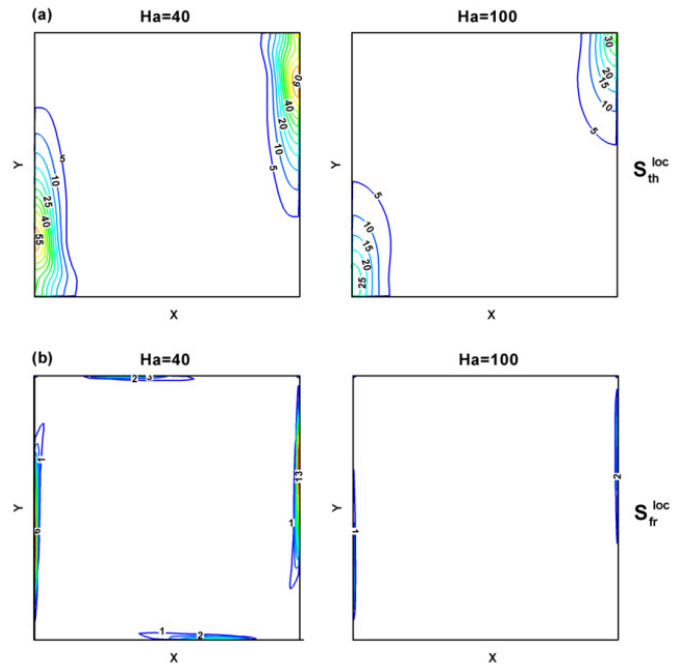


Fig. 10 Typical snapshots of local entropy generation contours for $Ha = 40$ and 100 ($Ri=100$ and $Pr = 0.025$): (a) Isocontours of thermal local entropy S_{th}^{loc} , and (b) structures of local entropy due to the fluid friction S_{fr}^{loc} .

Influence of Richardson parameter on the irreversibility phenomena

In order to highlight the effect of the Richardson number on the irreversibility criterion present in the cavity, the total entropy generation profile S_{tot} as well as that due to fluid friction and heat transfer S_{fr} and S_{th} are depicted in Fig. 11 for the fixed parameters ($Ha=100$ and $Pr=0.025$). Contrarily to the Hartmann parameter, augmenting the Richardson value leads to enhancing the irreversibility rates within the cavity filled with liquid gallium. In fact, the entropy generation remains almost constant for the first three lowest Richardson values $Ri=0.1, 1$ and 10 , after which the profiles undergo a significant increase for relatively highest value $Ri=100$. Moreover, the figure shows again that the entropy generation is dominated by thermal effects. This is explained by the very close values of S_{tot} and S_{th} . Moreover, smaller values of total entropy generation due to fluid friction S_{fr} were reported in this figure which demonstrates again that irreversibility criterion rate in the case of magnetoconvection mixed convection are less influenced by the viscous effects of the fluid.

4.2 Mixed convection for different cases of driving lids

In this section, we will predict the Hartmann effect on the flow structure, the thermal field and irreversibility criterion exhibited in the driven cavity filled with liquid gallium for different case of driving lids ($Ra = 4 \times 10^5$, $Gr = Ra / Pr = 1.6 \times 10^7$, $Ri = 100$, and $Pr = 0.025$). The first case corresponds to the situation where only the top wall is driven (case 1). The second and third cases correspond to the situation where both top and bottom horizontal walls move in the same (case 2) and opposite directions (case 3). In Fig. 12 (a) are shown the histograms relative to the variation of average Nusselt number versus various Hartmann number for the three cases investigated. As illustrated in this figure, the case 3 corresponding to the situation where both horizontal walls are driven in opposite directions appears to provide the optimal heat transfer and this for all Ha values. Moreover, we can see that driving both lids (cases 2 and 3) increases the value of the average Nusselt number compared to the case where a single wall is kept mobile (case 1). This may explained by the fact that a further moving accelerates the flow and thereby enhances the convection in the cavity causing the increase of heat transfer rate.

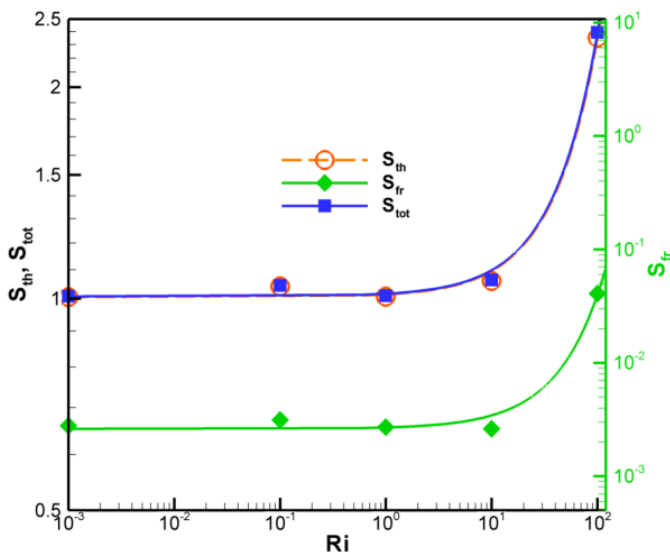


Fig. 11 Variations of the total entropy production due to fluid friction S_{fr} , due to heat transfer S_{th} and total entropy generation S_{tot} as a function of Richardson number Ri for $Ha = 100$ and $Pr = 0.025$.

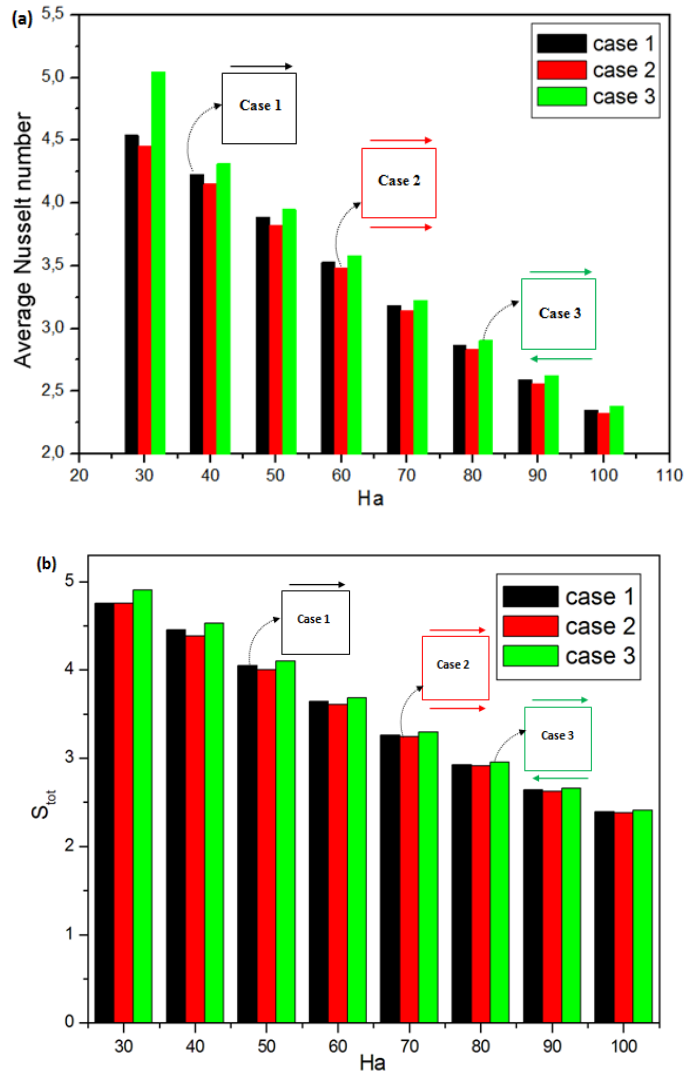


Fig. 12 Histograms of the average Nusselt number and total entropy generation as a function of the Ha values for the three cases investigated of lid driven cavities for $Pr=0.025$ and $Ri = 100$: (a) \overline{Nu} , and (b) S_{tot} .

On another hand, in order to quantify the irreversibility rate in the driven cavity according to all three cases considered, we illustrate in Fig. 12 (b) the variation of total entropy generation with the Hartmann number. This figure reflects that entropy generation seems to strengthen at the third case, and this is revealed in fair accordance with the variations of the average Nusselt number. This allows concluding that irreversibility phenomenon strongly depends on the heat transfer rate and thus can grow or diminish depending on the importance of the convection in the lid driven cavity filled with liquid metal.

5. CONCLUSION

The current study is concerned with the numerical simulation of magneto mixed convection and entropy generation phenomena within a lid driven square cavity filled with multiple liquid metals in the presence of a uniform magnetic field. Three situations of moving lid were considered in the current investigation. An in-house code based on finite volume method with the help of a full multigrid acceleration is implemented for the numerical computations. A code validation was firstly carried out with previously published studies on special cases of the considered problem and found to be in fair agreement. Effects of the main parameters; namely the Prandtl, Hartmann and Richardson

numbers as well as the lid driven situations on the heat transfer rate, thermal field and irreversibility phenomena were predicted and analyzed. For the first case were only the top lid is animated, it is determined that the magnetic field influence on the flow patterns and thermal field is manifested in general by reduction of the heat transfer rate for all liquid metals considered. Furthermore, for the cavity filled with liquid gallium, isotherm structures demonstrate that a conductive regime may occur and cause the birth of fluid trajectory deformations at the vicinity of the four cavity corners by strengthening the values of Hartmann number. Besides, the Richardson number effect is also discussed with the practical visualizations of velocity component profiles and stream traces. It is seen that the increase of Ri values leads to acceleration of the flow with a centro-symmetry that is exhibited according to all velocity component profiles. Besides, a correlation of average Nusselt number was established as a function of Ri parameter for the case of the single lid-driven cavity filled with liquid gallium. In terms of irreversibility phenomena, it was shown that both total entropy generation due to fluid friction and to heat transfer continues to lower by further augmenting the Hartmann number. Furthermore, it is found that entropy generation phenomena are dominated by the thermal irreversible effects in the lid driven cavity. On another hand, and contrarily to the Hartmann parameter, enhancing the Richardson number leads to strengthening the irreversibility rates within the cavity especially for relatively highest values while it has no significant effect for lower ones. Of particular interest is the comparison of the heat transfer and entropy generation criterion for different cases of driving lids. It was shown that the case where both horizontal walls are moving in opposite directions appears to provide the optimal heat transfer and to strengthen the irreversibility phenomena and this for all the values of Ha.

NOMENCLATURE

B_0	Magnitude of magnetic field
Be	Bejan number, $Be = S_{th} / (S_{th} + S_{fr})$
g	acceleration of gravity (m/s^2)
Gr	Grashof number, $Gr = g\beta(T_h - T_c)H^3 / \nu^2$
H	height of the enclosure (m)
Ha	Hartmann number, $Ha = B_0H\sqrt{\sigma / \rho\nu}$
k	conductivity ($J m^{-1} s^{-1} K^{-1}$)
Nu	local Nusselt number
\overline{Nu}	average Nusselt number, defined in Eq. (5)
P	dimensionless pressure
Pr	Prandtl number, ν / α
R	gas constant
Ra	Rayleigh number, $gH^3\beta(T_h - T_c) / \nu\alpha$
Re	Reynolds number, $Re = U_0H / \nu$
Ri	Richardson number, $Ri = Gr / Re^2$
S	dimensionless entropy generation
T_c	cold wall temperature (K)
T_h	hot wall temperature (K)
T	temperature (K)
t	dimensionless time
U, V	dimensionless velocity components in X, Y directions
U_0	lid velocity, m/s
X, Y	dimensionless Cartesian coordinates

Greek Symbols

α	thermal diffusivity (m^2/s)
β	coefficient of thermal expansion (K^{-1})
Δ	difference value

θ	dimensionless temperature, $\theta = (T - T_c) / (T_h - T_c)$
ν	kinematics viscosity (m^2/s)
μ	dynamic viscosity, ($Kg m^{-1} s^{-1}$)
ρ	fluid density (kg / m^3)
σ	electrical conductivity, ($\Omega^{-1}m^{-1}$)
Φ	generic variable (U, V, P or θ)
φ	irreversibility coefficient ratio
Ω	global domain

Subscripts

max	maximum
o	reference value or location
fr	friction
loc	local
th	thermal
tot	total

REFERENCES

- Al-Mudhaf, A., and Chamkha, A.J., 2004, "Natural Convection of Liquid Metals in an Inclined Enclosure in the Presence of a Magnetic Field," *International Journal of Fluid Mechanics Research*, **31**(3) 221-243.
<http://dx.doi.org/10.1615/InterJFluidMechRes.v31.i3.20>
- Abu-Nada, E., 2015, "Dissipative Particle Dynamics Simulation of Combined Convection in a Vertical Lid Driven Cavity with a Corner Heater," *International Journal of Thermal Sciences*, **92**, 72-84.
<https://doi.org/10.1016/j.ijthermalsci.2015.01.022>
- Al-Rashed, Abdullah A.A.A., Kolsi, L., Kalidasan, K., Maatkid, C., Borjini, M. N., Aichouni, Mohamed and P. R., Kanna, 2017, "Effect of Magnetic Field Inclination on Magnetoconvective Induced Irreversibilities in a CNT-water Nanofluid Filled Cubic Cavity," *Frontiers in Heat and Mass Transfer (FHMT)*, **8**, 003031
<http://dx.doi.org/10.5098/hmt.8.31>
- Botella, O., and Peyret, R., 1998, "Benchmark Spectral Results on the Lid-driven Cavity Flow," *Computers & Fluids*, **27**, 421-433.
[https://doi.org/10.1016/S0045-7930\(98\)00002-4](https://doi.org/10.1016/S0045-7930(98)00002-4)
- Brown, D.L., Cortez, R., and Minion, M.L., 2001, "Accurate Projection Methods for the Incompressible Navier-Stokes Equations," *Journal of Computational Physics*, **168**, 464-499.
<https://doi.org/10.1006/jcph.2001.6715>
- Ben-Cheikh, N., Ben-Beya, B., and Lili, T., 2007, "Benchmark Solution for Time-Dependent Natural Convection Flows with an Accelerated Full-Multigrid Method," *Numerical Heat Transfer, Part B: Fundamentals*, **52**, 131-151.
<http://dx.doi.org/10.1080/10407790701347647>
- Ben-Beya, B., and Lili, T., 2009, "Transient Natural Convection in 3D Tilted Enclosure Heated from Two Opposite Sides," *International Communications in Heat and Mass Transfer*, **36**, 604-613.
<https://doi.org/10.1016/j.icheatmasstransfer.2009.02.014>
- Bezi, S., Ben-Cheikh, N., Ben-Beya, B., and Taeb, L., 2015, "Enhancement of Natural Convection Heat Transfer Using Different Nanoparticles in an Inclined Semi-Annular Enclosure Partially Heated from Above," *High Temperature*, **53**(1), 99-117.
<http://dx.doi.org/10.1134/S0018151X15010022>

Cheng, T.S., 2011, "Characteristics of Mixed Convection Heat Transfer in a Lid-Driven Square Cavity with Various Richardson and Prandtl Numbers," *International Journal of Thermal Sciences*, **50**, 197-205.
<https://doi.org/10.1016/j.ijthermalsci.2010.09.012>

E. Erturk, 2009, "Discussions on Driven Cavity Flow, *Int. J. Numer. Methods Fluids*, **60**(3), 275-294.
<http://dx.doi.org/10.1002/flid.1887>

Farid, S.K., Billah, M. M., Rahman, M. M., and Sharif, Uddin Md., 2013, "Numerical Study of Fluid Flow on Magneto-Hydrodynamic Mixed Convection in a Lid Driven Cavity Having a Heated Circular Hollow Cylinder," *Procedia Engineering*, **56**, 474-479.
<https://doi.org/10.1016/j.proeng.2013.03.149>

Hayase, T., Humphrey, J.A.C., and Greif, R., 1992, "A Consistently Formulated QUICK Scheme for Fast and Stable Convergence using Finite-Volume Iterative Calculation Procedures," *Journal of Computational Physics*, **98**, 108-118.
[https://doi.org/10.1016/0021-9991\(92\)90177-Z](https://doi.org/10.1016/0021-9991(92)90177-Z)

Hadjidimos, A., 2000, "Successive Overrelaxation (SOR) and Related Methods," *Journal of Computational and Applied Mathematics*, **123**, 177-199.
[https://doi.org/10.1016/S0377-0427\(00\)00403-9](https://doi.org/10.1016/S0377-0427(00)00403-9)

Iwatsu, R., Hyun, J.M., and Kuwahara, K., 1993, "Mixed Convection in a Driven Cavity with a Stable Vertical Temperature Gradient," *International Journal of Heat and Mass Transfer* **36**, 1601-1608.
[https://doi.org/10.1016/S0017-9310\(05\)80069-9](https://doi.org/10.1016/S0017-9310(05)80069-9)

Kolsi, L., Hussein, A. K., Borjini, M. N., Mohammed, H. A., and Ben Aïssia, H., 2014, "Computational Analysis of Three-Dimensional Unsteady Natural Convection and Entropy Generation in a Cubical Enclosure Filled with Water-Al₂O₃ Nanofluid," *Arab. J. Sci. Eng.*, **39**(11), 7483-7493.
<http://dx.doi.org/10.1007/s13369-014-1341-y>

Kefayati, G.H.R., 2014, "Simulation of Magnetic Field Effect on Natural Convection of Non-Newtonian Power-Law Fluids in a Sinusoidal Heated Cavity using FDLBM," *International Communications in Heat and Mass Transfer* **53**, 139-153.
<https://doi.org/10.1016/j.icheatmasstransfer.2014.02.026>

Kefayati, G.H. R., 2015, "FDLBM Simulation of Magnetic Field Effect on Mixed Convection in a Two Sided Lid-Driven Cavity Filled with Non-Newtonian Nanofluid," *Powder Technology*, **280**, 135-153.
<https://doi.org/10.1016/j.powtec.2015.04.057>

Kefayati, G.H. R., 2015, "Magnetic Field Effect on Heat and Mass Transfer of Mixed Convection of Shear-Thinning Fluids in a Lid-Driven Enclosure with Non-Uniform Boundary Conditions," *Journal of the Taiwan Institute of Chemical Engineers*, **51**, 20-33.
<https://doi.org/10.1016/j.jtice.2015.01.006>

Kefayati, G.H.R., 2015, "FDLBM Simulation of Entropy Generation due to Natural Convection in an Enclosure Filled with Non-Newtonian Nanofluid," *Powder Technology*, **273**, 176-190.
<https://doi.org/10.1016/j.powtec.2014.12.042>

Kolsi, L., 2016, "MHD Mixed Convection and Entropy Generation in a 3d Lid-Driven Cavity," *Frontiers in Heat and Mass Transfer (FHMT)*, **7**, 013026.
<http://dx.doi.org/10.5098/hmt.7.26>

Lin, L., Chen, Yi-C., Lin, Chao-A., 2011, "Multi Relaxation Time Lattice Boltzmann Simulations of Deep Lid Driven Cavity Flows at Different Aspect Ratios," *Computers & Fluids*, **45**(1), 233-240.

<https://doi.org/10.1016/j.compfluid.2010.12.012>

Mohamad, A. A., and Viskanta, R., 1994, "Flow Structures and Heat Transfer in a Lid-Driven Cavity Filled with Liquid Gallium and Heated from Below," *Experimental Thermal and Fluid Science*, **9**, 309-319.
[https://doi.org/10.1016/0894-1777\(94\)90033-7](https://doi.org/10.1016/0894-1777(94)90033-7)

Mukhopadhyay, A., 2010, "Analysis of Entropy Generation due to Natural Convection in Square Enclosures with Multiple Discrete Heat Sources," *International Communications in Heat and Mass Transfer*, **37**, 867-872.
<https://doi.org/10.1016/j.icheatmasstransfer.2010.05.007>
Magherbi, M., Abbassi, H., Hidouri, N., and Ben Brahim, 2006, A., "Second Law Analysis in Convective Heat and Mass Transfer," *Entropy*, **8**, 1-17.
<http://dx.doi.org/10.3390/e8010001>

Mahmoudi, A., Mejri, I., Abbassi, M. A., and Omri, A., 2014, "Lattice Boltzmann Simulation of MHD Natural Convection in a Nanofluid-Filled Cavity with Linear Temperature Distribution," *Powder Technology*, **256**, 257-271.
<https://doi.org/10.1016/j.powtec.2014.02.032>

Mahmoudi, A., Mejri, I., Abbassi, M. A., and Omri, A., 2014, Analysis of the Entropy Generation in a Nanofluid-Filled Cavity in the Presence of Magnetic Field and Uniform Heat Generation/Absorption," *Journal of Molecular Liquids*, **198**, 63-77.
<https://doi.org/10.1016/j.molliq.2014.07.010>

Mehrez, Z., El Cafsi, A., Belghith, A., and Le Quééré, P., 2015, "MHD Effects on Heat Transfer and Entropy Generation of Nanofluid Flow in an Open Cavity," *Journal of Magnetism and Magnetic Materials*, **374**, 214-224.
<https://doi.org/10.1016/j.jmmm.2014.08.010>
Naffouti, A., Ben-Beya, B., and Lili, T., 2014, "Three-Dimensional Rayleigh-Bénard Magnetoconvection: Effect of the Direction of the Magnetic Field on Heat Transfer and Flow Patterns," *Comptes Rendus Mécanique*, **342**, 714-725.
<https://doi.org/10.1016/j.crme.2014.09.001>

Oreper, G. M. and Szekely, J., 1983, "The Effect of an Externally Imposed Magnetic Field on Buoyancy Driven Flow in a Rectangular Cavity," *Journal of Crystal Growth*, **64**, 505-515.
[https://doi.org/10.1016/0022-0248\(83\)90335-4](https://doi.org/10.1016/0022-0248(83)90335-4)

Ouertatani, N., Ben Cheikh, N., Ben Beya, B., Lili, T., Campo, A., 2009, "Mixed Convection in a Double Lid-Driven Cubic Cavity," *International Journal of Thermal Sciences*, **48**, 1265-1272.
<https://doi.org/10.1016/j.ijthermalsci.2008.11.020>

Oztop, H. F., and Al-Salem, K., I. Pop, 2011, "MHD Mixed Convection in a Lid-Driven Cavity with Corner Heater," *International Journal of Heat and Mass Transfer*, **54**, 3494-3504.
<https://doi.org/10.1016/j.ijheatmasstransfer.2011.03.036>

Oueslati, F., Ben-Beya, B., and Lili, T., 2011, "Aspect Ratio Effects on Three-Dimensional Incompressible Flow in a Two-Sided Non-Facing Lid-Driven Parallelepiped Cavity," *Comptes Rendus Mécanique* **339**, 655-665.
<https://doi.org/10.1016/j.crme.2011.06.002>

Oueslati, F., Ben-Beya, B., and Lili, T., 2013, Double-Diffusive Natural Convection and Entropy Generation in an Enclosure of Aspect Ratio 4 with Partial Vertical Heating and Salting Sources, *Alexandria Engineering Journal*, **52**, 605-625.
<https://doi.org/10.1016/j.aej.2013.09.006>

Oueslati, F., Ben-Beya, B., and Lili, T., 2014, "Numerical Simulation of Unsteady Double-Diffusive Natural Convection within an Inclined Parallelepipedic Enclosure," *International Journal of Modern Physics C*, **25**, 1450058.

<https://doi.org/10.1142/S0129183114500582>

Oueslati, F., Ben-Beya, B., and Lili, T., 2014, "Numerical Investigation of Thermosolutal Natural Convection in a Rectangular Enclosure of an Aspect Ratio Four with Heat and Solute Sources," *Heat Mass Transfer*, **50**, 721–736.

<http://dx.doi.org/10.1007/s00231-013-1280-2>

Oueslati, F., Ben-Beya, B., and Lili, T., 2015, "Some Aspects of the Three-Dimensional Double-Diffusive Natural Convection in a Parallelepipedic Tilted Solar Distiller," *International Letters of Chemistry, Physics and Astronomy*, **55**, 47-58.

<http://dx.doi.org/10.18052/www.scipress.com/ILCPA.55.47>

Rudraiah, N., Barron, R.M., Venkatachalappa, M., and Subbaraya, C.K., 1995, "Effect of a Magnetic Field on Free Convection in a Rectangular Enclosure," *International Journal of Engineering Science* **33**, 1075-1084.

[https://doi.org/10.1016/0020-7225\(94\)00120-9](https://doi.org/10.1016/0020-7225(94)00120-9)

Sathiyamoorthy, M., and Chamkha, A., 2010, "Effect of Magnetic field on Natural Convection Flow in a Liquid Gallium Filled Square Cavity for Linearly Heated Side Wall(s)," *International Journal of Thermal Sciences*, **49**, 1856-1865.

<https://doi.org/10.1016/j.ijthermalsci.2010.04.014>

Sathiyamoorthy, M., and Chamkha, A.J., 2012, "Natural Convection Flow Under Magnetic Field in a Square Cavity for Uniformly (or) Linearly Heated Adjacent Walls," *Int. J. Numer. Meth. for Heat & Fluid Flow*, **22**, 677-698.

<https://doi.org/10.1108/09615531211231307>

Sheikholeslami, M., G-Bandpy, M., Ganji, D.D., and Soleimani, S., 2013, "Effect of a Magnetic Field on Natural Convection in an Inclined Half-Annulus Enclosure Filled with Cu–Water Nanofluid using CVFEM," *Advanced Powder Technology*, **24**(6) 980–991.

<https://doi.org/10.1016/j.apt.2013.01.012>

Wang, L.B., and Wakayama, N. I., 2002, "Dependence of Aspect Ratio on Magnetic Damping of Natural Convection in Low-Conducting Aqueous Solution in a Rectangular Cavity," *International Journal of Heat and Fluid Flow*, **23**, 92.95.

[https://doi.org/10.1016/S0142-727X\(01\)00138-2](https://doi.org/10.1016/S0142-727X(01)00138-2)

Yazdi, M. E., Moradi, A., and Dinar and, S., 2014, "MHD Mixed Convection Stagnation-Point Flow Over a Stretching Vertical Plate in Porous Medium Filled with a Nanofluid in the Presence of Thermal Radiation," *Arabian Journal for Science and Engineering*, **39**(3), 2251-2261.

<http://dx.doi.org/10.1007/s13369-013-0792-x>

Zahmatkesh, I., 2008, "On the Importance of Thermal Boundary Conditions in Heat Transfer and Entropy Generation for Natural Convection Inside a Porous Enclosure," *International Journal of Thermal Sciences*, **47**, 339–346.

<https://doi.org/10.1016/j.ijthermalsci.2007.02.008>